Numerical Simulations of Tropospheric Heating Effects on the Quasi-biennial Oscillation

John Noble
Meteorology 205A
December 12, 2006
(Revised, 2024)

Abstract

The effects of tropospheric heating on the quasi-biennial oscillation (QBO) are examined using a two-dimensional mechanistic model of the equatorial stratosphere. Tropospheric heating is simulated by increasing the amplitudes of vertically-propagating Kelvin and Rossby-gravity waves. Both observations and theoretical analysis have identified that vertically propagating equatorial Kelvin and Rossby-gravity waves drive the westerly and easterly QBO regimes respectively. Amplitudes for both waves are increased linearly in 2% increments, resulting in non-linear decreases in period and non-linear increases in westerly velocity maxima (up to 16%).

Introduction

The quasi-biennial oscillation (QBO) is an oscillation of easterly and westerly stratospheric zonal wind regimes with a period range of 22–34 months and a mean period of 28 months (Baldwin *et al.* 2001; Holton 2004). Maximum amplitudes of > 40 m s^{-1} are found above the equator at 20 mb, and decrease by 50% by 12°N and S latitude. Alternating wind regimes appear above 30 km and propagate downward at 1 km $month^{-1}$, maintaining amplitude until 23 km, and losing amplitude below 23 km (Holton 2004). The westerly regime duration is greater than the easterly at lower levels, while the easterly regime duration is greater than westerly at upper levels. Easterly magnitudes are predominantly greater than the westerly magnitudes (Cordero and Nathan 2000; Holton 2004).

Both observations and theoretical analysis have identified that vertically propagating equatorial Kelvin and Rossby-gravity waves drive the westerly and easterly QBO regimes respectively (Holton 2004). The QBO is a unique dynamical phenomenon in that its period is seemingly unrelated to the periods of these driving waves (Baldwin 2001).

This paper presents results from 2.5-D model simulations of the effects of tropospheric warming on the QBO. Warming was simulated by increasing the amplitudes of Kelvin and Rossby-gravity waves.

Model Description

Model dynamics are based on Takahasi (1987). Cordero and Nathan (2000) extended the model by coupling the wave and zonal mean ozone continuity equations to the wave and zonal mean temperature equations respectively through diabatic heating terms. This enables the model to simulate the effects of the wave fields on the zonal mean circulation (Cordero and Nathan 2000). Dependent variables are divided into zonal mean and two wave components, a wave-1 ($k = 1$) Kelvin wave and a wave-4 ($k = 4$) Rossby-gravity wave. Mean components are represented with an overbar, and wave components with primes. All equations use standard notation found in Takahashi (1987), Holton (2004), and Cordero and Nathan (2000).

The zonal mean equations include:

$$\frac{\partial \overline{u}}{\partial t} + \overline{v}\frac{\partial \overline{u}}{\partial y} + \overline{w}\frac{\partial \overline{u}}{\partial z} - \beta y \overline{v} = -\frac{\partial}{\partial y}\left(\overline{u'v'}\right) - \frac{1}{\rho}\frac{\partial}{\partial z}\left(\overline{\rho u'w'}\right) + \nabla_D^2 \overline{u}, \tag{1}$$

$$\frac{\partial \overline{v}}{\partial t} + \beta y \overline{u} = -\frac{\partial \overline{\Phi}}{\partial y} + \nabla_D^2 \overline{v}, \tag{2}$$

$$\frac{\partial \overline{v}}{\partial y} + \frac{1}{\rho}\frac{\partial\left(\rho \overline{w}\right)}{\partial z} = 0, \tag{3}$$

$$\frac{\partial \overline{\Phi}_z}{\partial t} + \overline{v}\frac{\partial \overline{\Phi}_z}{\partial y} + \overline{w}\frac{\partial \overline{\Phi}_z}{\partial z} + N^2 \overline{w} = -\frac{\partial\left(\overline{v'\Phi'_z}\right)}{\partial y} - \alpha_N\left(\overline{\Phi}_z\right) + A\overline{\gamma} + \nabla_D^2 \overline{\Phi}_z. \tag{4}$$

Geopotential is related to temperature by

$$T = \frac{H}{R}\frac{\partial \Phi}{\partial z}. \tag{5}$$

The above equations are zonal mean prognostic equations: (1) *u*-momentum; (2) *v*-momentum; (3) mass continuity; (4) geopotential, which can be used as a prognostic equation for temperature due to (5). The first term on the right-hand side (RHS) of (4) is northward heat flux.

Circulation in the model is driven by the geopotential height of equatorial Kelvin and Rossby-gravity waves at the lower boundary represented by

$$\Phi'_K = A_K e^{\left(-\beta y^2/2c_K\right)} \mathrm{Re}\left[e^{ik_K(x-c_K t)} \right], \tag{6}$$

$$\Phi'_R = A_R y \left(\frac{\beta m_R}{N} \right)^{1/2} e^{-\frac{\beta |m_R| y^2}{2N}} \times \mathrm{Re}\left[e^{ik_R(x-c_R t)} \right], \tag{7}$$

where the subscripts *K* and *R* refer to the Kelvin and Rossby-gravity waves respectively. Wave-mean flow interactions occur in (1), where the zonally averaged meridional and vertical momentum flux terms affect the mean flow.

Methods

The effects of tropospheric warming on the QBO were simulated by varying the Kelvin and Rossby-gravity wave amplitudes (A_K , A_R). As a first order simulation, five model runs were conducted in which the amplitudes of both the Kelvin and Rossby-gravity waves were increased successively by 2% from the RS values (Table 1).

Table 1. Run parameters

Run number	Percent increase from RS	Rossby-gravity wave Amplitude (m^2 s^{-2})	Kelvin wave Amplitude (m^2 s^{-2})
RS	0	300	204
1	2	306	208
2	4	312	212
3	6	318	216
4	8	324	220
5	10	330	224

In the tropics, higher surface and tropospheric temperatures (due to increasing levels of atmospheric CO_2) are thought to increase condensation and latent heat release, which in

turn lead to increased total potential energy. In a number of global simulations with CO_2 levels doubled and surface temperatures increased by 5.1 C, Rind *et al.* (1998) reported that 1000–100 mb total potential energy increased by 2%, and zonal available energy increased from 4.1–28.5%. In addition, they found an increase in stratospheric eddy energy and residual circulation on the order of 50-70% for the annual average at 25 km. These residual circulation increases were driven by an increase in Eliassen-Palm (EP) flux convergences caused by changes in wave propagation into the stratosphere due to warming in the upper tropical troposphere (Rind *et al.* (1998). Therefore, since Kelvin and Rossby-gravity waves are excited by oscillations in large scale convective heating in the equatorial troposphere (Holton 2004), the amplitude variations listed in Table 1 seemed to be reasonable for a first order simulation.

Results

Zonal wind, temperature, and ozone QBO plots were generated to compare the different runs. Figure **1** shows overlays of the five runs for the above three quantities. The zonal wind QBO indicates that the westerly regime's maximum velocities increased with increasing run number, from 29.35 to 33.18 m s^{-1} for runs 1 to 5 respectively while the easterly regime's maximum velocities decreased in magnitude from -28.84 to -25.74 for runs 1 to 5 respectively (Tables 2 and 3). The mean *u*-wind QBO amplitude, however, increased only slightly, from 29.07 to 29.46 m s^{-1} for runs 1 to 5 respectively, reflecting the symmetric trend of increasing westerly and decreasing easterly magnitudes for all runs. Period changes in the temperature and ozone QBOs were similar to those seen in the *u*-wind QBOs (Figure **1**). The above changes can also be seen in Figure **4** and 5: time-height cross sections of zonal wind for runs 1-5 (westerly winds are represented in red, easterly in blue).

Table 2. Zonal wind statistics, Runs 1–5

QBO Cycle	Run # & K & RG Wave Amplitude Increment (%)	U-wind Easterly max ($m\ s^{-1}$)	Time (years)	U-wind Westerly max ($m\ s^{-1}$)	U-wind Westerly Diff (%)	U-wind QBO Amp. ($m\ s^{-1}$)	Time (years)	U-wind QBO Period (Easterly) (yr.dec)	U-wind QBO Period (Westerly) (yr.dec)	Mean U-wind QBO period (yr.dec)	U-wind QBO Period Diff. (%)
1	RS (0)	-28.94	2.19	28.26	0.00	28.60	0.88				
1	Run 1 (2)	-28.82	2.08	28.80	1.94	28.81	0.85				
1	Run 2 (4)	-27.77	2.00	30.23	6.98	29.00	0.79				
1	Run 3 (6)	-26.71	1.92	31.55	11.66	29.13	0.77				
1	Run 4 (8)	-25.87	1.84	32.59	15.35	29.23	0.74				
1	Run 5 (10)	-25.71	1.75	32.98	16.71	29.34	0.74				
2	RS (0)	-28.93	4.55	28.91	0.00	28.92	3.23	2.36	2.36	2.36	0.00
2	Run 1 (2)	-28.83	4.38	29.44	1.82	29.13	3.12	2.30	2.27	2.29	-2.91
2	Run 2 (4)	-27.73	4.22	30.76	6.40	29.25	3.04	2.22	2.25	2.23	-5.23
2	Run 3 (6)	-26.68	4.08	32.00	10.66	29.34	2.96	2.16	2.19	2.18	-7.56
2	Run 4 (8)	-25.86	3.97	32.92	13.85	29.39	2.90	2.14	2.16	2.15	-8.72
2	Run 5 (10)	-25.73	3.84	33.11	14.50	29.42	2.82	2.08	2.08	2.08	-11.63
3	RS (0)	-28.92	6.93	28.95	0.00	28.94	5.59	2.38	2.36	2.37	0.00
3	Run 1 (2)	-28.81	6.68	29.49	1.85	29.15	5.42	2.30	2.30	2.30	-2.89
3	Run 2 (4)	-27.75	6.47	30.82	6.45	29.28	5.26	2.25	2.22	2.23	-5.78
3	Run 3 (6)	-26.69	6.27	32.03	10.62	29.36	5.12	2.19	2.16	2.18	-8.09
3	Run 4 (8)	-25.84	6.08	33.07	14.22	29.45	5.01	2.11	2.11	2.11	-10.98
3	Run 5 (10)	-25.75	5.92	33.20	14.69	29.48	4.88	2.08	2.05	2.07	-12.72
4	RS (0)	-28.93	9.29	28.94	0.00	28.94	7.97	2.36	2.38	2.37	0.00
4	Run 1 (2)	-28.82	8.96	29.52	2.01	29.17	7.70	2.27	2.27	2.27	-4.05
4	Run 2 (4)	-27.75	8.68	30.79	6.40	29.27	7.51	2.22	2.25	2.23	-5.78
4	Run 3 (6)	-26.67	8.44	32.08	10.84	29.37	7.32	2.16	2.19	2.18	-8.09
4	Run 4 (8)	-25.85	8.22	32.97	13.93	29.41	7.15	2.14	2.14	2.14	-9.83
4	Run 5 (10)	-25.74	7.97	33.35	15.25	29.55	6.96	2.05	2.08	2.07	-12.72
5	RS (0)	#N/A	#N/A	28.96	0.00	#N/A	10.33	#N/A	2.36	2.36	0.00
5	Run 1 (2)	#N/A	#N/A	29.52	1.92	#N/A	10.00	#N/A	2.30	2.30	-2.33
5	Run 2 (4)	-27.74	10.90	30.81	6.38	29.28	9.73	2.22	2.22	2.22	-5.82
5	Run 3 (6)	-26.69	10.63	32.08	10.77	29.39	9.51	2.19	2.19	2.19	-6.98
5	Run 4 (8)	-25.86	10.36	33.03	14.03	29.44	9.29	2.14	2.14	2.14	-9.31
5	Run 5 (10)	-25.76	10.05	33.25	14.82	29.50	9.01	2.08	2.05	2.07	-12.21

Table 3. Mean values

Run #	Mean Easterly max ($m\ s^{-1}$)	Mean Westerly max ($m\ s^{-1}$)	Mean U-wind Amplitude ($m\ s^{-1}$)	Mean QBO Period (yr.dec)
RS	-28.93	28.80	28.85	
1	-28.84	29.35	29.07	2.36
2	-27.75	30.68	29.22	2.29
3	-26.69	31.95	29.32	2.23
4	-25.86	32.92	29.39	2.18
5	-25.74	33.18	29.46	2.13

Figure **2** shows the percent increase of the westerly regimes' velocity maxima as a function of run number. The solid line represents a linear increase from 0 to 10%, while the dots represent the maximum westerly velocity percent increase from the RS for the five QBO cycles in the 11-year simulation. While run 1 displays a near linear velocity increase for the five cycles, with percent increases from 1.94 to 1.92, runs 2–5 display non-linear velocity maxima increases for each of the five QBO cycles, with the greatest

deviation (from linear) occurring in the first QBO cycle of run 5 (16.7 % increase). Figure **3** shows the percent decrease of zonal wind QBO periods as a function of run number, indicating a non-linear change in almost all cases.

These non-linear changes appear to be a result of the non-linear, coupled, equations which govern the mean flow. Changes in the wave amplitude via equations (6) and (7) affect (4) which in turn affects the zonal flow in (1) via $\overline{v}$ and $\overline{w}$.

Discussion

Both observations and theoretical analysis have determined that vertically propagating Kelvin and Rossby-gravity waves provide a significant portion of the momentum required to drive the QBO with Kelvin waves transferring westerly momentum and Rossby-gravity waves transferring easterly momentum (Holton 2004). The consistent increase in westerly winds and decrease in easterly winds is an interesting result. This may be a function of how the model is tuned, resulting in Kelvin waves dominating Rossby-gravity waves (Cordero and Nathan 2000). Further simulations which isolate the effects of both Kelvin and Rossby-gravity waves are required to better understand these dynamics.

Figure 1. Zonal mean wind, temperature deviation, and ozone volume mixing ratio anomaly, Height 25 K, Latitude 0° N (Runs 1–5)

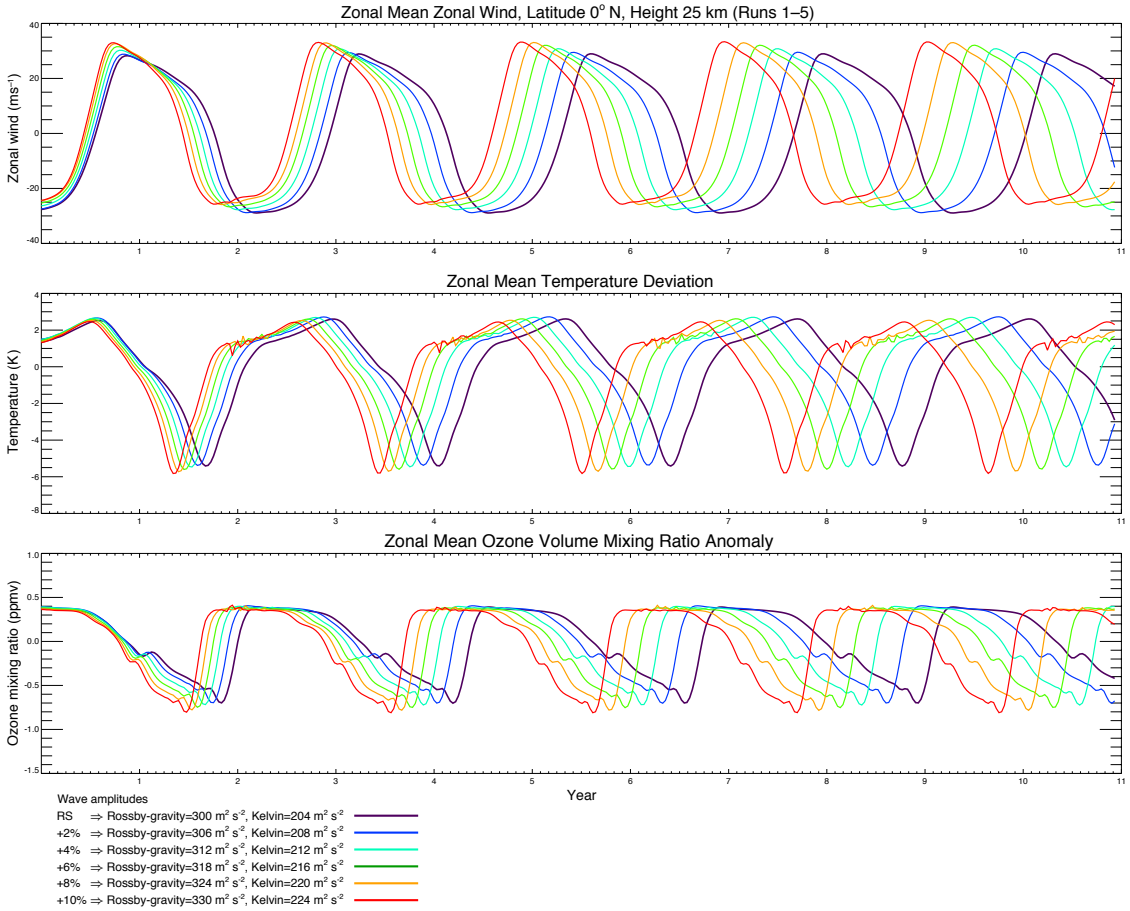

Figure 2. Percent increase of westerly regimes' velocity maxima as a function of run number

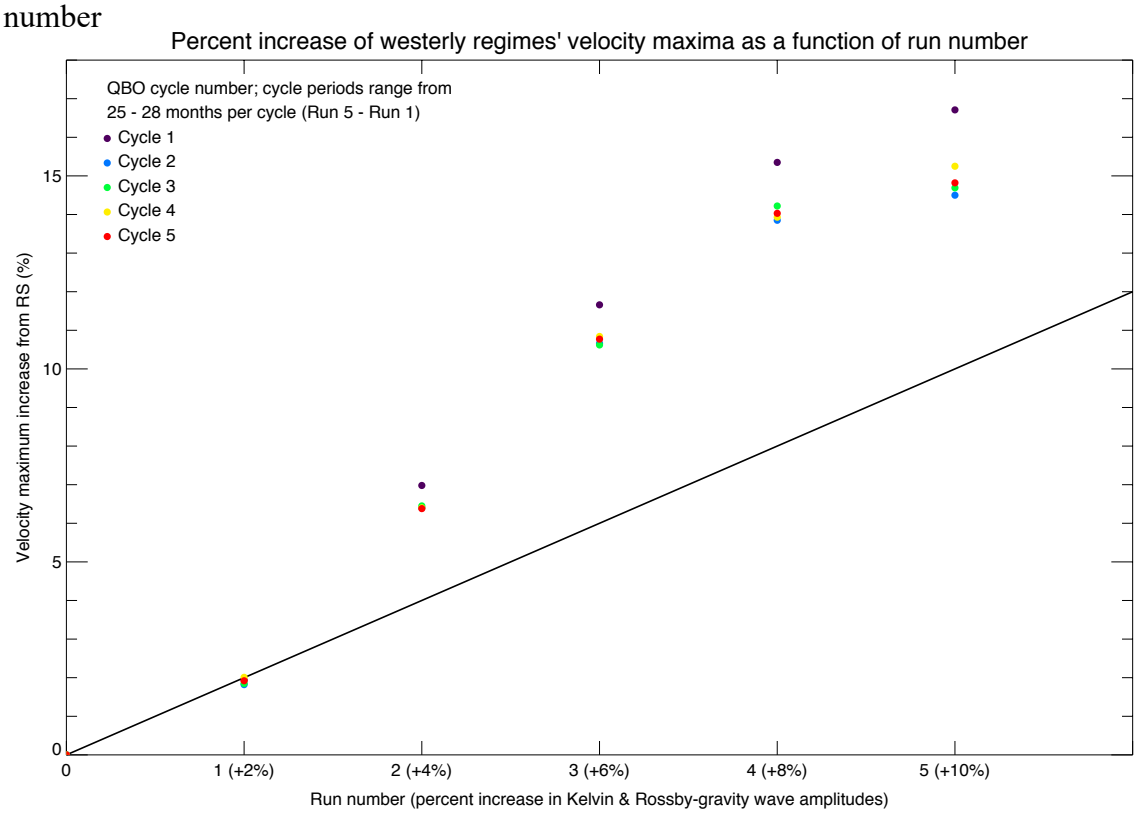

Figure 3. Percent decrease of zonal wind QBO periods as a function of run number

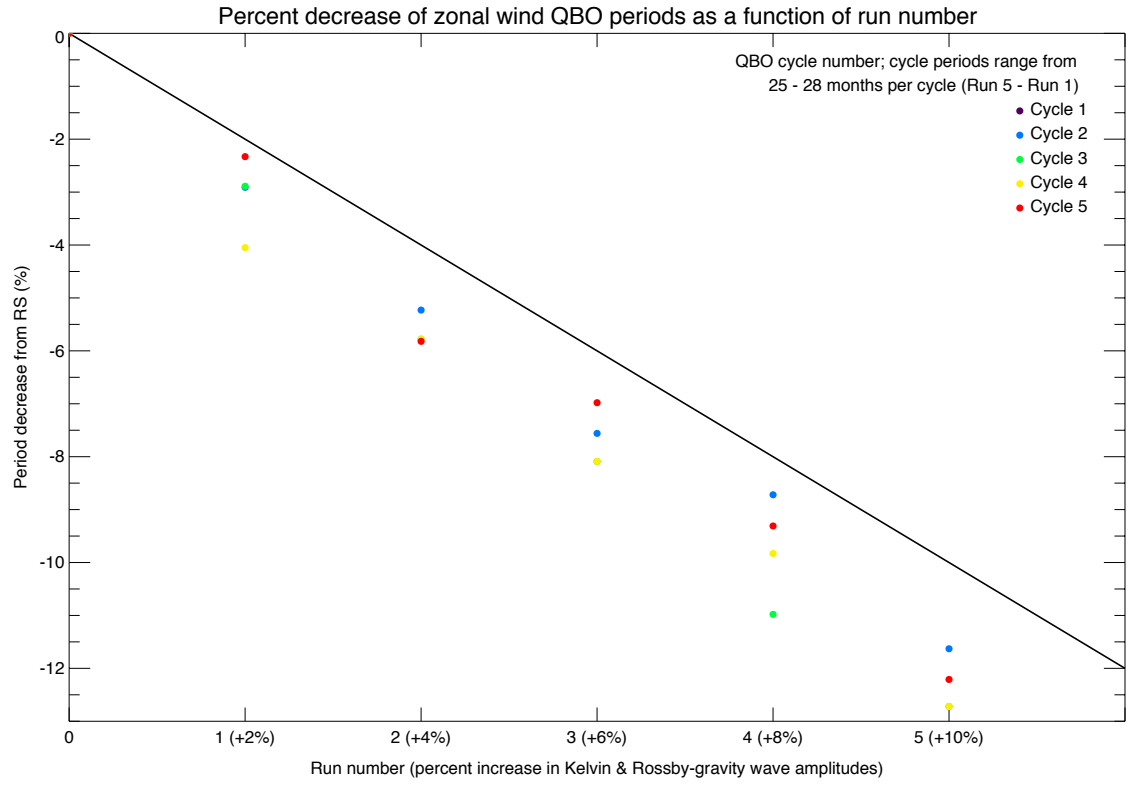

Figure 4. Time-height cross sections of zonal wind (Runs 1 & 2)

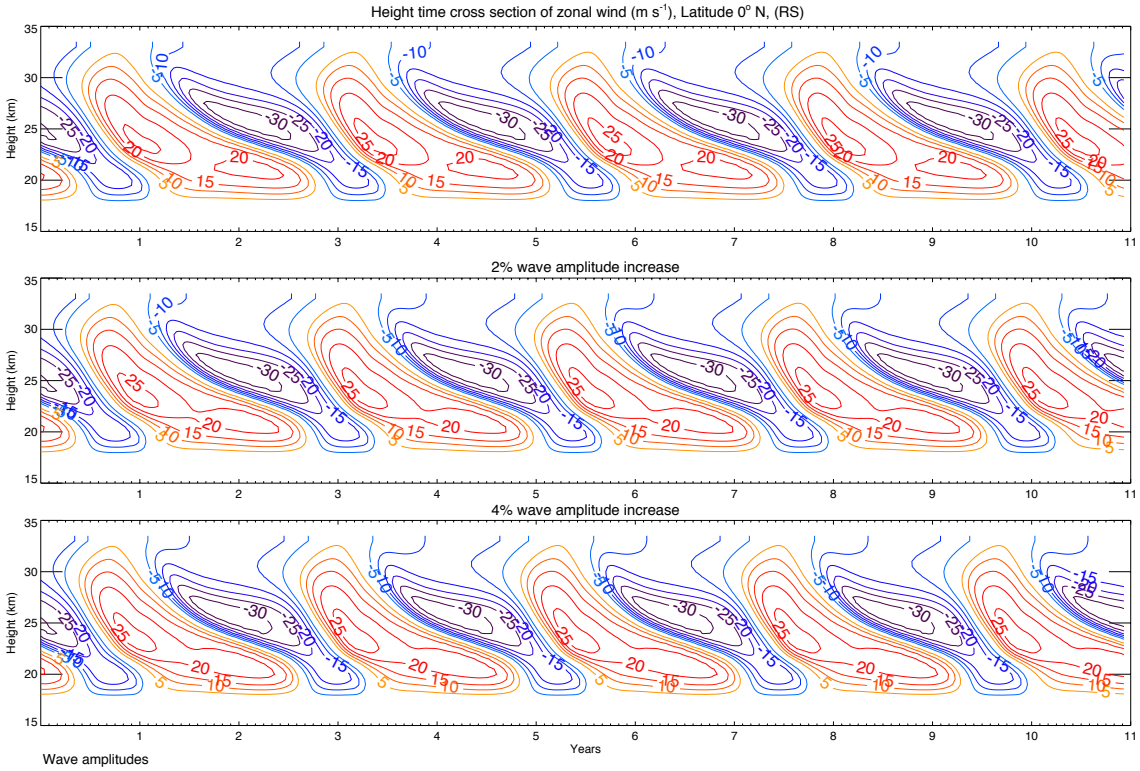

Wave amplitudes
Rossby-gravity=300 $m^2 s^{-2}$, Kelvin=204 $m^2 s^{-2}$ (RS)
Rossby-gravity=306 $m^2 s^{-2}$, Kelvin=208 $m^2 s^{-2}$ (+2%)
Rossby-gravity=312 $m^2 s^{-2}$, Kelvin=212 $m^2 s^{-2}$ (+4%)

Figure 5. Time-height cross sections of zonal wind (Runs 3–5)

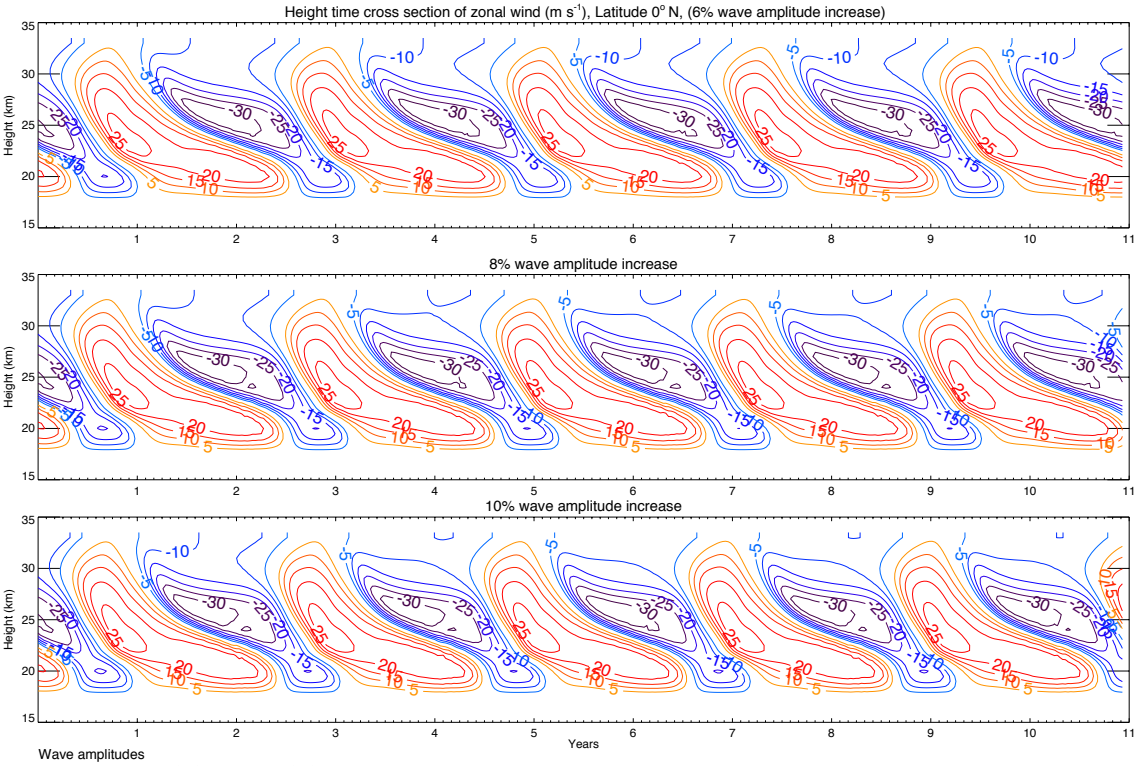

Wave amplitudes
Rossby-gravity=318 $m^2 s^{-2}$, Kelvin=216 $m^2 s^{-2}$ (+6%)
Rossby-gravity=324 $m^2 s^{-2}$, Kelvin=220 $m^2 s^{-2}$ (+8%)
Rossby-gravity=330 $m^2 s^{-2}$, Kelvin=224 $m^2 s^{-2}$ (+10%)

Figure 6. Fast Fourier transform power spectra of zonal wind, Latitude 0° N (Runs 1–5)

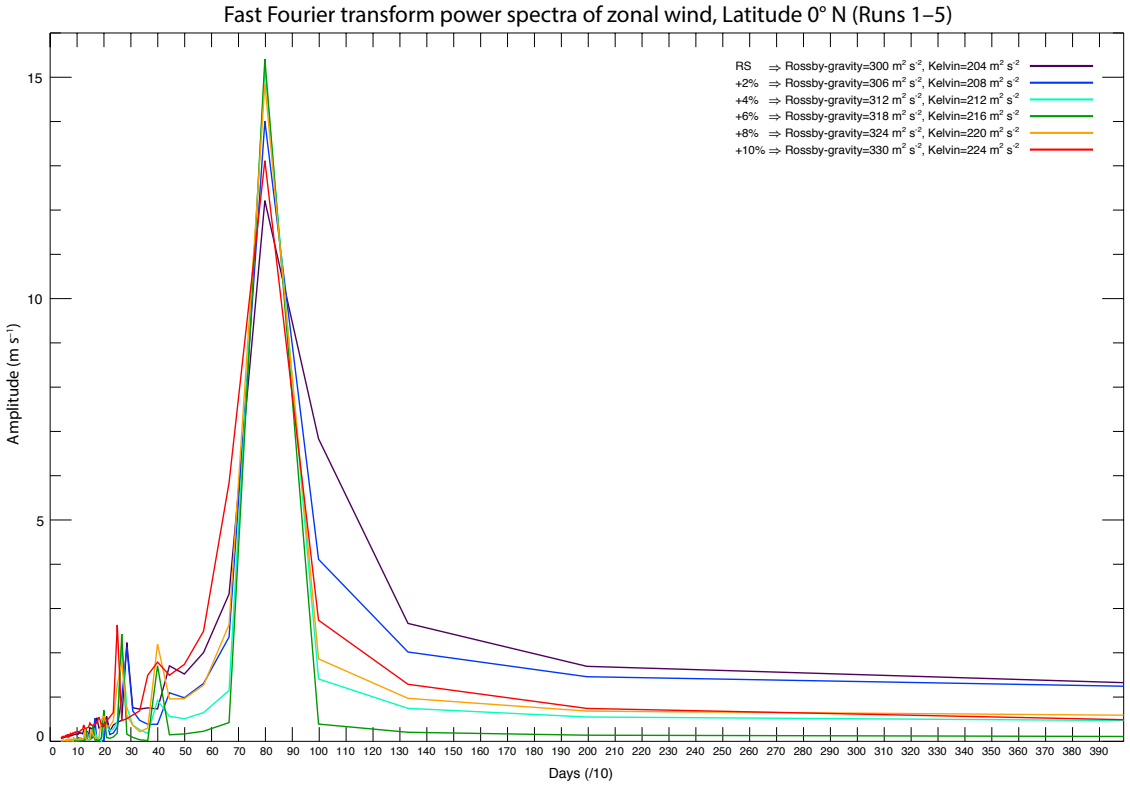

References

Andrews, D. G., J. R. Holton, and C. B. Leovy, 1987: Middle Atmosphere Dynamics. Academic Press Inc., Orlando, FL.

Baldwin, M. P., L. J. Gray, T. J. Dunkerton, K. Hamilton, P. H. Haynes, W. J. Randel, J. R. Holton, M. J. Alexander, I. Hirota, T. Horinouchi, D. B. A. Jones, J. S. Kinnersley, C. Marquardt, K. Sato, and M. Takahashi, 2001: The quasi-biennial oscillation. *Rev. Geophys.,* **39**, 179–229.

Cordero, E. C., and T. R. Nathan, 2000: The Influence of Wave- and Zonal Mean-Ozone Feedbacks on the Quasi-biennial Oscillation. *J. Atmos. Sci.,* **57**, 3426–3442.

Holton, J.R. and Lindzen, R.S., 1972: An updated theory for the quasi-biennial cycle of the tropical stratosphere. *J. Atmos. Sci.,* **29**, 1076–1080.

Holton, J. R., 2004: An introduction to dynamic meteorology. Elsevier Academic Press, 529 pp.

Rind, D., D. Shindell, P. Lonergan, N. K. Balachandran, 1998: Climate change and the middle atmosphere. Part III: The doubled CO2 climate revisited. *J. Climate*, **11**, 876–894.

Takahashi, M., 1987: A 2-dimensional numerical model of the quasi-biennial oscillation: Part I. *J. Meteor. Soc. Japan*, **65**, 523–536.

Takahashi, M., B. A. Boville, 1992: A three-dimensional simulation of the equatorial quasi-biennial oscillation. *J. Atmos. Sci.,* **49**, 1020–1035.